6-2004

Polystyrene Magadiite Nanocomposites

Dongyan Wang
Marquette University

David D. Jiang
Marquette University

Jaclyn Pabst
Marquette University

Zhidong Han
Beijing Institute of Technology

Jianqi Wang
Beijing Institute of Technology

See next page for additional authors

Polystyrene Magadiite Nanocomposites

DONGYAN WANG,[1] DAVID D. JIANG,[1] JACLYN PABST,[1]
ZHIDONG HAN,[2] JIANQI WANG,[2] *and* CHARLES A. WILKIE[1]

[1]*Department of Chemistry*
Marquette University
P.O. Box 1881, Milwaukee, WI 53201-1881

[2]*School of Chemical Engineering and Materials Science*
Beijing Institute of Technology
100081, Beijing, China

An organically modified magadiite has been prepared and used to make a mixed intercalated-exfoliated polystyrene nanocomposite by bulk polymerization. This system gives excellent improvement in mechanical properties, but the thermogravimetric analysis curves do not show any change in the onset of the degradation and the degradation pathway is not changed from that for virgin polystyrene, unlike the situation for an aluminosilicate clay, montmorillonite. By cone calorimetry, the peak heat release rate is not changed, again unlike the results with the aluminosilicate. This suggests that not all clays exhibit the same behavior in nanocomposite formation. Polym. Eng. Sci. 44:1122–1131, 2004. © 2004 Society of Plastics Engineers.

INTRODUCTION

Polymer nanocomposites have been the subject of extensive research in recent years. There is an expectation that the presence of layered silicate materials, e.g. montmorillonite, hectorite, bentonite, etc., at low loading levels, 3%–5%, can greatly improve the mechanical properties, enhance the barrier properties and improve the fire retardancy of polymers (1–6). Most interest has been focused on montmorillonite systems and less attention has been directed to layered silicic acids (7–11), such as magadiite.

Magadiite, named in 1967 after the locality of its discovery near Lake Magadi, Kenya, is one of the layered silicates with the general formula $NaSi_7O_{13}(OH)_3{\cdot}3H_2O$. Because a single crystal has not been obtained, the crystal structure is still unknown. Three main structures have been proposed: a tetrahedra with two inverted tetrahedra forming a six-member ring (12); a five-member ring combination structure similar to that in zeolite (13); and a five-member and six-member ring combination with silica tetrahedra chains (14).

These silicates usually have excess negative charge, which is balanced by the exchangeable cations in the gallery space. Like montmorillonite clay, the cation exchangeability offers the possibility for the modification of pristine magadiite (Na-magadiite, H-magadiite) by organic cations, which can increase the organophilic character of the gallery space so that it is compatible with an organic polymer. Because of the outstanding performance of montmorillonite clay in the enhancement of barrier properties and in fire retardancy, there is an interest to compare magadiite to montmorillonite to determine what affects the performance of clays. There are differences between the two clays in terms of cation exchange capacity but the major difference is that montmorillonite is an aluminosilicate, while magadiite contains only silicate.

Binette and Detellier (15) used H-magadiite into which had been intercalated aprotic solvents, such as dimethylsulfoxide, N-methylformamide and hexamethylphosphorictriamide; they have intercalated poly(ethylene glycols) into this material at 150°C. There is no structural change in the magadiite, as shown by ^{29}Si NMR, and the d-spacing increases by only 0.4 nm. Isoda (16) prepared covalently bound polymers in the interlayer space by grafting α-methacryloxypropylsilyl groups on dodecyltrimethylammonium-exchanged magadiite and then copolymerized this with methyl methacrylate (MMA). This is different from the traditional polymer nanocomposite, in which the ionic interaction between silicate and organic modifiers dominates.

Primary, secondary, tertiary and quaternary onium ions were used to form the organically modified magadiite, which was then used to form intercalated and exfoliated nanocomposites by *in-situ* polymerization (17, 18). Elongation at break and tensile strength were both improved, which is opposite to the conventional

Published online in Wiley InterScience (www.interscience.wiley.com).
DOI: 10.1002/pen.20105

composite behavior. The transparency of the exfoliated magadiite hybrid is an especially notable property. Acrylonitrile was *in-situ* polymerized in the gallery of dodecyltrimethylammonium (C12) ion modified magadiite by Sugahara (19) to investigate the possibility of using polyacrylonitrile intercalated magadiite as a precursor for the synthesis of non-oxide ceramics by the carbothermal reduction method. Ogawa (20) reported an azobenzene-magadiite intercalation compound by photochromic reactions for controlling the microstructure to construct photofunctional supramolecular systems. After the ion-exchange reaction, the basal spacing increased from 1.57 nm to 2.69 nm, which suggested two possible orientations of the intercalant in the gallery; namely in the monomolecular layer or in the bilayer inclined to the silicate sheets.

In this paper, we report the studies on the cation exchange process, solvent effects on organic modification of magadiite and the formation of styrene nanocomposites using an organically modified salt, which has also been used with montmorillonite.

EXPERIMENTAL

Materials. Dimethylhexadecylamine (≥ 98%) was acquired from Fluka. The majority of the other chemicals used in this study, including vinylbenzyl chloride (97%), monomeric styrene, benzoyl peroxide (BPO) 97% and tetrahydrofuran (THF) (99+%), were purchased from the Aldrich Chemical Company. The polymerization inhibitor was removed from the monomer by passing it through an inhibitor-remover column, also acquired from Aldrich. Distilled water was used throughout.

Modification of Magadiite. Two different methods were used for the organo-modification of magadiite, which are called herein the THF method and H_2O method; these were adapted from the literature method (17). The cationic exchange reaction occurs between sodium magadiite and a quaternary ammonium salt, in this case, styryldimethylhexadecylammonium chloride (VB16) was utilized (21). For the THF method, 5 grams of sodium magadiite was predispersed in 200 ml THF over 24 hrs using magnetic stirring at room temperature, and then a 10% mole excess of the VB16 salt (based on the CEC of the magadiite) was used for the cationic exchange reaction. After 24 h the reaction was stopped, the mother liquor was removed by centrifugation, and then reaction was resumed by adding fresh ammonium salt. This procedure was repeated twice; the products from these procedures are indicated as 1×, 2× and 3×, respectively. For the H_2O method, all the procedures are the same except that THF was replaced by H_2O. Finally, the modified magadiite was dried in a vacuum oven at room temperature. The literature method was also used for comparison; in this method the cationic exchange process was performed twice, each time with 24 h as the exchange period. Further details are available elsewhere (17).

Preparation of Nanocomposite. A bulk polymerization technique was utilized in the preparation of the polystyrene (PS) magadiite nanocomposite. This procedure, which has been used for montmorillonite, has been previously described (21, 22).

Instrumentation. X-ray diffraction (XRD) pattern were obtained using a Rigaku Geiger Flex, 2-circle powder diffractometer equipped with Cu Kα generator (λ = 1.5404 Å). Generator tension was 50 kV and generator current was 20 mA. Bright field transmission electron microscopy (TEM) images of the composites were obtained at 60 kV with a Zeiss 10c electron microscope. The samples were ultramicrotomed with a diamond knife on a Reicher-Jung Ultra-Cut E microtome at room temperature to create sections ~70 nm thick. The sections were transferred from the knife-edge to 600 hexagonal mesh Cu grids. Thermogravimetric analysis (TGA) was performed on a Cahn TG-131 unit under a 30 mL/min flowing nitrogen atmosphere at a scan rate of 10°C/min from room temperature to 600°C; temperatures are reproducible to ±3°C, and the fraction of nonvolatile materials is reproducible to ±3%. TGA/FTIR studies were carried out using the Cahn thermogravimetric analyzer coupled to a Mattson Research grade FTIR. Mechanical properties were measured using Reliance RT/5 (MTS System Corporation) for material testing at a crosshead speed of 0.05 in/min; the reported values are the average of five determinations. The samples for mechanical testing were prepared by injection molding using an Atlas model CS 183MMX Mini-Max molder. Cone calorimetry was performed on an Atlas CONE2 according to ASTM E 1354-92 at an incident flux of 35 kW/m^2 using a cone shaped heater. Exhaust flow was set at 24 l/s and the spark was continuous until the sample ignited. Cone samples were prepared by compression molding the sample (about 30 g) into square plaques. Typical results from Cone calorimetry are reproducible to within about ±10%. These uncertainties are based on many runs in which thousands of samples have been combusted (23). The XPS experiments were carried out as previously described (24–27), using the pseudo *in-situ* technique in which the sample is heated outside of the XPS chamber under an argon atmosphere. During the analysis the sample orientation must be kept unchanged from beginning to end. The spectra were obtained using a Perkin-Elmer PHI 5300 ESCA system at 250 W (12.5 kV at 20 mA) under a vacuum better than 10^{-6} Pascal (10^{-8} Torr). The spectrometer was calibrated using the binding energy of adventitious carbon as 284.6 eV. The samples were prepared by solvent casting a thin film from tetrahydrofuran (THF) solution onto aluminum foil. The d-spacing of the nanocomposites before and after dissolution was determined and no change was found.

RESULTS AND DISCUSSION

X-ray Diffraction (XRD). The layered structure of magadiite and its nanocomposite were characterized by XRD through the peak position shifts and the intensity changes. *Figure 1* shows that after the cationic exchange

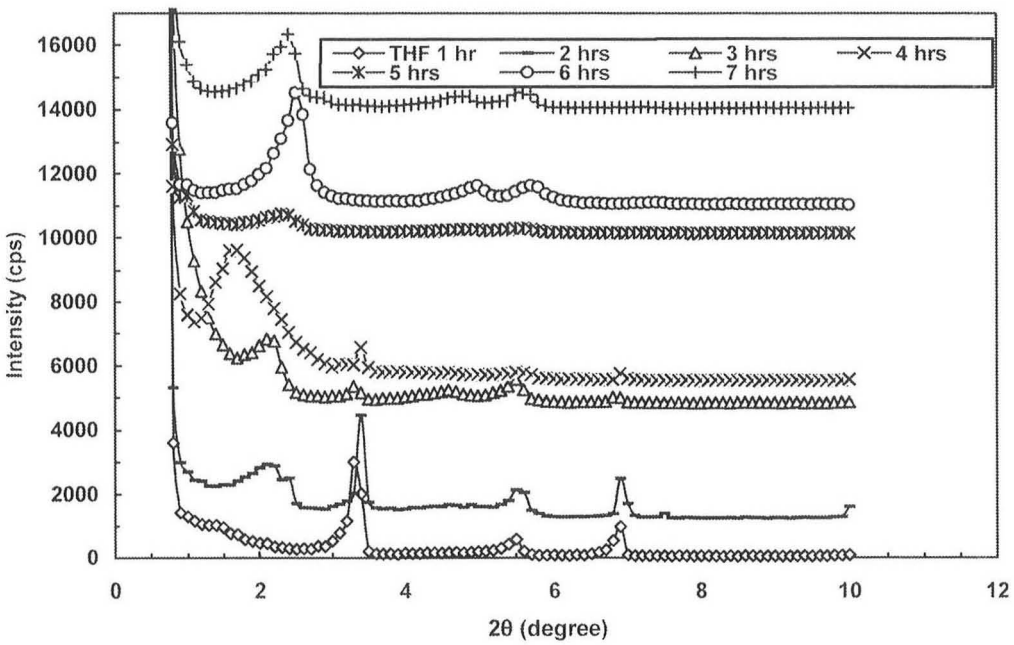

Fig. 1. XRD traces for the cation exchange in THF for various time periods.

reaction, the peak positions all shifted to lower 2θ value, indicating that the interlayer of sodium magadiite was intercalated by the long chain ammonium salt. The 001 peak position shifted from high 2θ value to low 2θ value, 3.3° at 1 h, 2.1° at 2 h, 2.1° at 3h and 1.7° at 4 h exchange, which corresponds to 2.7 nm, 4.2 nm, 4.2 nm and 5.2 nm, respectively. When the exchange time is longer than 4 h, the position shifts to higher 2θ values. Over the time period between 5 h to several weeks, the 2θ is in the range of 2.3°~2.5°, corresponding to a d-spacing 3.5 to 3.8 nm; these results are all shown in *Table 1*. The cation exchange process is relatively slow and the return to lower d-spacing probably indicates that the highest d-spacing is a meta-stable situation.

Solvent Effects on the Intercalation of Magadiite: THF vs. H_2O. *Figure 2* compares the XRD results for the THF vs. the H_2O method for the modification of magadiite. Cation exchange twice in pure water (2× H_2O method) is the literature method and this gives the smallest d-spacing 3.2 nm, pure THF and THF combined with water (THF/H_2O) method give a larger value, 3.7 nm. This implies that organic solvent THF has the better opportunity to promote the intercalation of the ammonium salt into the gallery space of magadiite. Observations with montmorillonite in these laboratories have suggested that there is no solvent effect in the ion exchange.

Table 1. Cationic Exchange Hours on the d-Spacing Shifts in THF.

Exchange Hours	2θ (degree)	d_{001} (nm)
1 hr	3.3	2.7
2 hrs	2.1	4.2
3 hrs	2.1	4.2
4 hrs	1.7	5.2
5 hrs	2.3	3.8
6 hrs	2.5	3.5
7 hrs	2.4	3.7
> 7 hrs	2.3	3.8
Several weeks	2.3	3.8

Figure 3 shows the effect on the d-spacing of the various exchange times with fresh ammonium salt in THF. A peak at 2θ = 5.7°, which is the position in pristine magadiite, is still present after one exchange; after two or three exchanges this peak completely disappears. This peak can be more clearly seen at 2θ = 6°, (*Fig. 4*) when the singly exchanged magadiite was used to prepare a polystyrene (PS) nanocomposite by bulk polymerization; this peak is not evident when the three times exchanged magadiite was used to prepare the nanocomposite. This clearly indicates that the magadiite is better dispersed after multiple exchanges than after only one exchange.

Comparing the water with the THF exchange, the observations from XRD are that peaks are present in the H_2O method, suggesting that intercalation has occurred, while they are absent in the THF method, perhaps suggesting that an exfoliated structure was obtained. These results suggest that the solvent used for the cation exchange has an important role in the type of nanocomposite that is obtained.

Transmission Electron Microscopy (TEM). The layered structure of the PS-magadiite nanocomposite was directly observed by TEM, as shown in *Figs. 5, 6* and *7*. In the low-magnification images of *Figs. 5* and *6*, there is evidence of the large platelets of magadiite, which indicates that this is not a well-dispersed system. In the high-magnification images, one can clearly

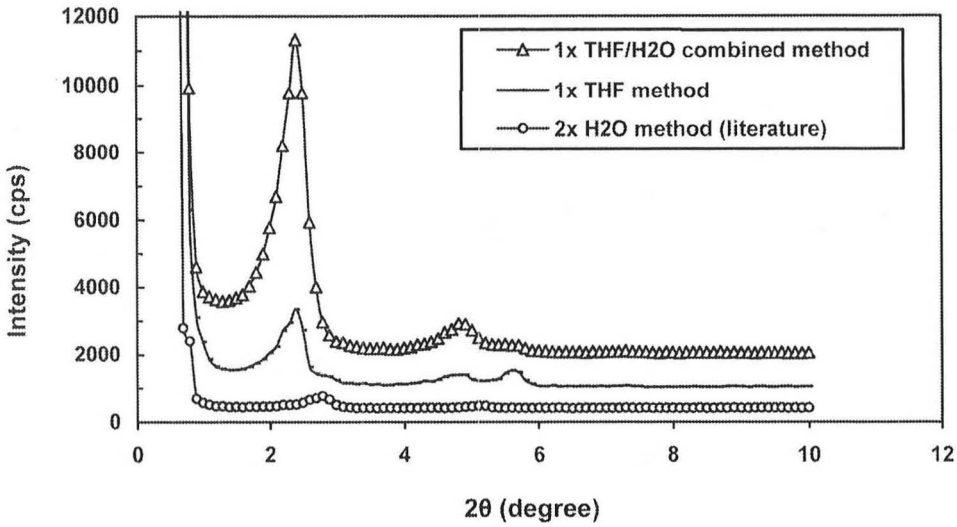

Fig. 2. Solvent effects on the cationic exchange, THF vs. H_2O.

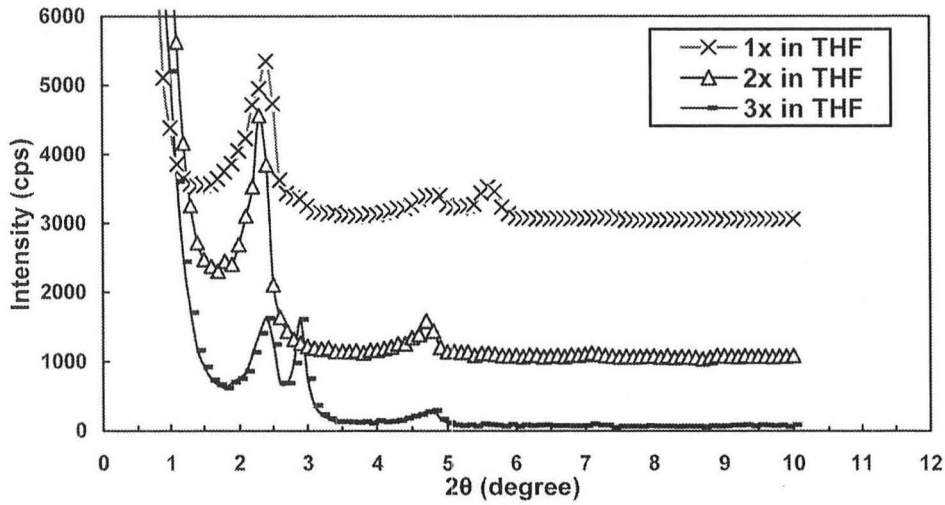

Fig. 3. The effect of the number of exchanges on the XRD traces.

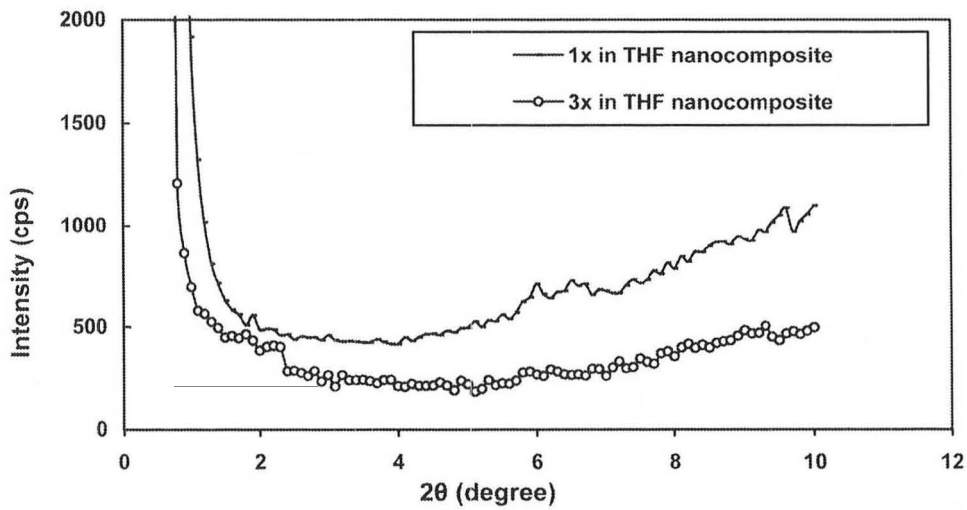

Fig. 4. Nanocomposite XRD traces from the THF method with one and three exchanges.

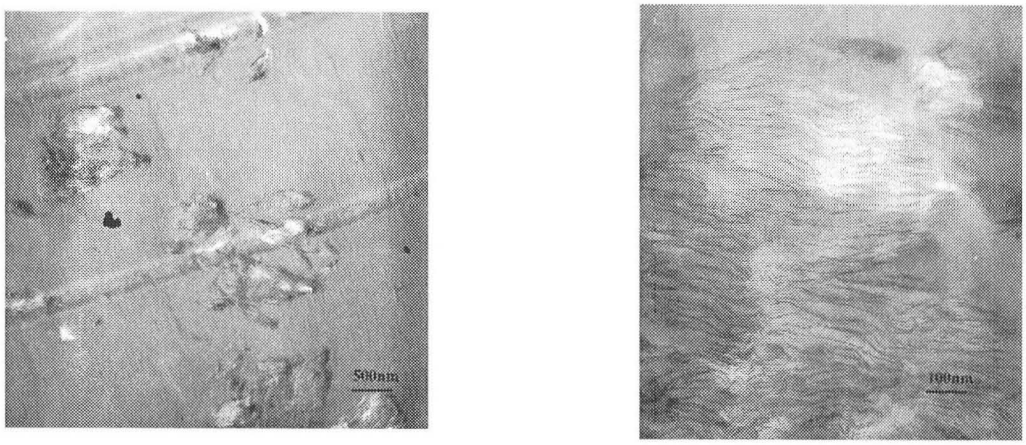

Fig. 5. TEM images of PS Magadiite nanocomposite from THF method: left is low magnification and right is the high magnification image.

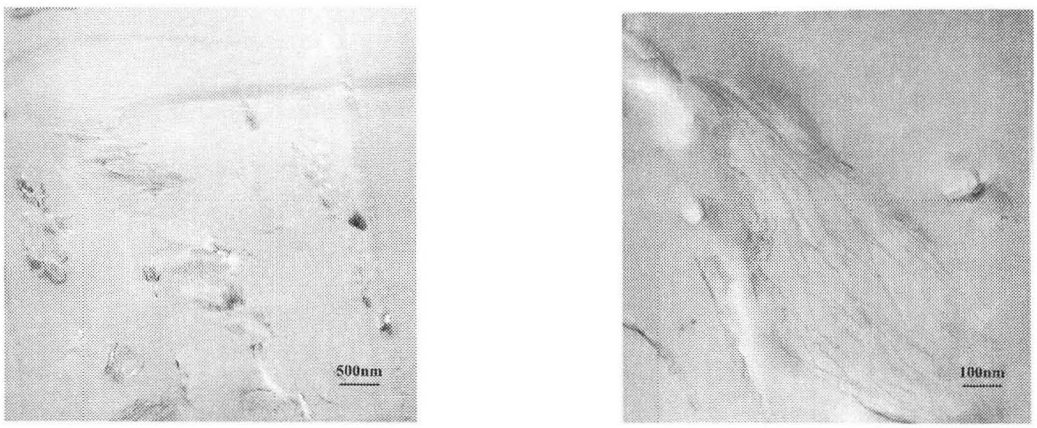

Fig. 6. TEM images of PS Magadiite nanocomposite from H_2O method: left is low magnification and right is the high magnification image.

see evidence for delamination of the material that was prepared using the THF method, while the H_2O method gives a mixture of exfoliation and intercalation. The image in *Fig. 7* is the high-magnification image of the nanocomposite that was obtained when the magadiite was only exchanged once in THF. This clearly shows the presence of clay tactoids, in agreement with the XRD results which show a peak at $2\theta = 6.0°$, the same position as seen in un-exchanged magadiite. This will give an immiscible component to the nanocomposite. The best description of this system is that it is a mixed nanocomposite that contains immiscible, intercalated and exfoliated components.

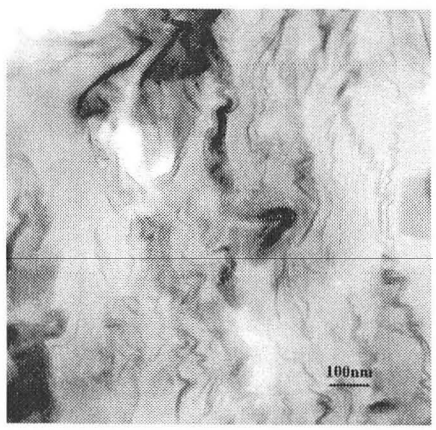

Fig. 7. TEM image at high magnification of PS magadiite nanocomposite from bulk polymerization using the singly exchanged clay by the THF method.

Mechanical Properties. Mechanical properties have been evaluated and the results are shown in *Table 2*. It is most commonly found that the mechanical properties, especially the modulus, of montmorillonite-polymer nanocomposites are increased (1). There is an expectation that the mechanical properties will always be improved for nanocomposites, but this has not been observed for some polymers (22). For the magadiite-polymer systems, the situation may be a little different, because magadiite has a larger plate area than montmorillonite clay, so the modulus improvement could be easily achieved; the tensile strength improvement may also be obtained because the larger plate provides a stronger interaction. Compared to virgin PS, sodium magadiite does not improve the mechanical properties

Table 2. Mechanical Properties of PS Magadiite Nanocomposite.

Sample	Modulus (GPa)	Peak Stress (MPa)
Pure PS	2.6	4.8
Maga-PS, bulk	2.1	3.7
Maga-VB16-PS, H_2O, bulk	3.5	22.4
Maga-VB16-PS, H_2O, bulk, 3×	3.7	17.6
Maga-VB16-PS, THF, bulk	4.0	11.6
Maga-VB16-PS, THF, bulk, 3×	3.7	14.7

of PS; this may be ascribed to the poor dispersion of the non-organically modified clay in the polymer matrix. The significant observation is that the organically modified magadiite does give greatly enhanced mechanical properties, regardless of the method used for modification.

Thermogravimetric Analysis (TGA) and Thermogravimetric Analysis—Fourier Transform Infrared Spectroscopy (TGA/FTIR). The thermal stability of the nanocomposites has been studied by TGA. The results for 3× exchanged magadiite PS nanocomposites are shown in *Table 3*; the data that is presented includes the temperature at which 10% degradation occurs, a measure of the onset of the degradation, the temperature at which 50% degradation occurs, the midpoint of the degradation, and the fraction of material that remains at 600°C, denoted as char. There is no change in the onset temperature for the PS nanocomposites compared to the pure PS; this result is quite different from that observed with montmorillonite, in which an increase in the onset temperature of 50°C is normal (21). This suggests that there may be a large difference between magadiite and montmorillonite.

Table 3. TGA Results for PS Magadiite Nanocomposites With 3× Washed Magadiite Prepared Samples.

Sample	10% Mass Loss, °C	50% Mass Loss, °C	Char (%) at 600°C
Pure PS	351	404	0
H_2O method, 3×	353	418	3
THF method, 3×	344	416	6

TGA/FTIR was used to identify the products of the degradation and thus provide a better understanding of the degradation pathway. *Figures 8* and *9* show the infrared spectra of 3× THF and 3× H_2O magadiite PS nanocomposites as a function of the temperature at which the volatiles are evolved. In previous work from these laboratories, it was shown that in the presence of montmorillonite clay, monomer formation is retarded (IR peak at 1630 cm^{-1}), while oligomer (1600 cm^{-1}) is produced (28). The TGA/FTIR data clearly show the presence of both monomer and oligomer in relatively similar amounts, suggesting that the presence of magadiite does not affect the course of the degradation in the same way as does montmorillonite.

X-ray Photoelectron Spectroscopy (XPS). Previously, XPS studies on polymer nanocomposites derived from aluminosilicate (29, 30) have been reported; XPS enables one to probe the surface of the degrading system and identify what is present at the surface. As a montmorillonite-polymer system undergoes degradation, carbon is lost from the surface, and oxygen, silicon, and aluminum accumulate, thereby confirming the barrier mechanism that has been proposed by Gilman (31) to account for the enhanced thermal stability of polymer-clay nanocomposites.

Figures 10, *11* and *12* show the changes in the surface amounts of carbon, oxygen and silicon, respectively, as

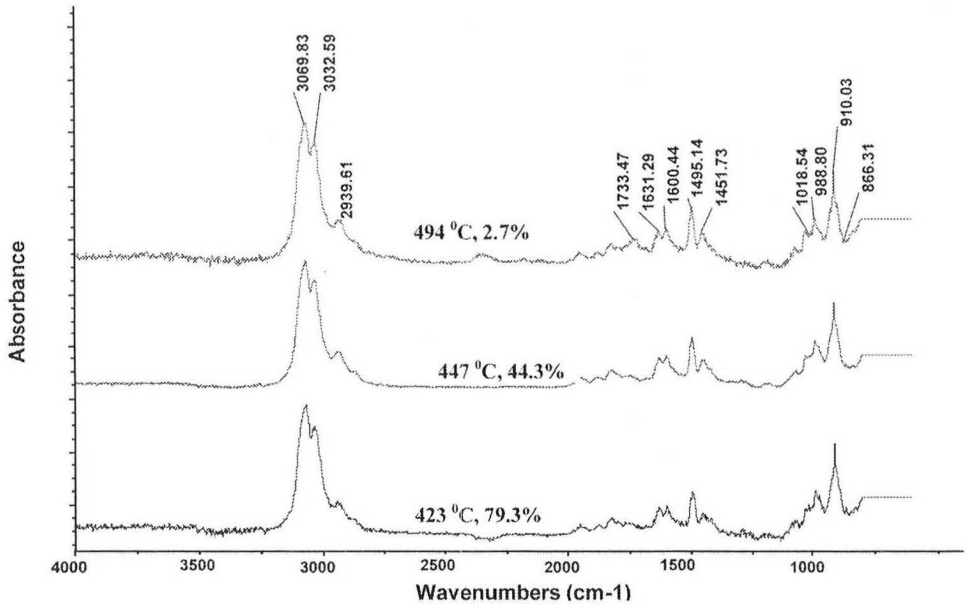

Fig. 8. TGA-FTIR plot on PS Magadiite nanocomposite, H_2O method, 3× exchanged.

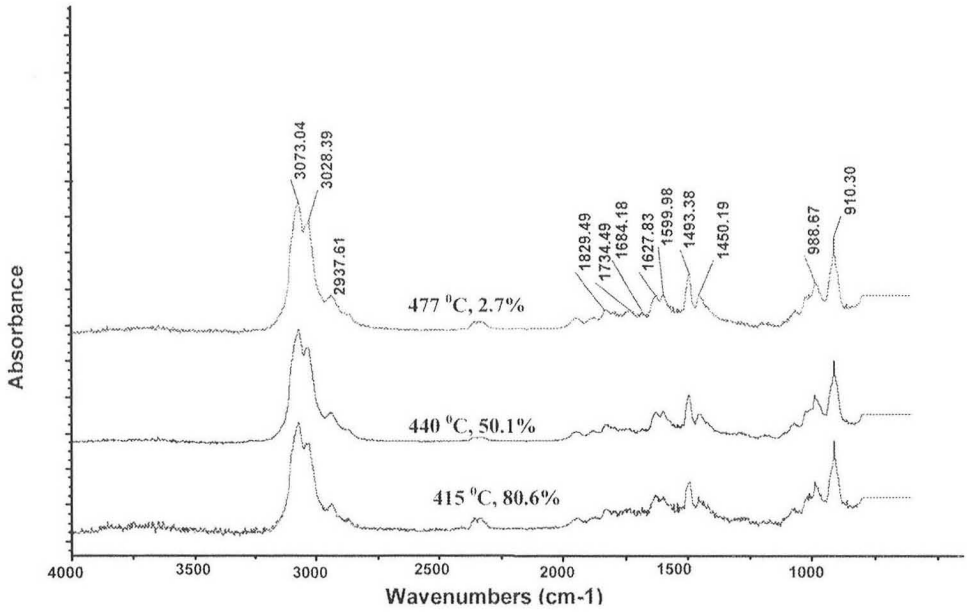

Fig. 9. TGA-FTIR plot on PS Magadiite nanocomposite, THF method, 3× exchange.

a function of temperature. Dramatic changes are seen for each element, all starting at the same temperature, 410°C. It is apparent that, just as with the montmorillonite systems, the polymer is lost from the surface and clay accumulates. Moreover, the binding energy of the silicon fluctuates around 102.5 eV, which is the value in magadiite, up to a temperature of 410°C. Above this temperature, the binding energy rises to 103.4 eV, a typical value for SiO_2. It is clear from this data that the silicate does form a barrier, as is also seen for montmorillonite nanocomposites.

Cone Calorimetry. The fire properties of the nanocomposites were assessed by cone calorimetry. The various parameters that may be evaluated using cone calorimetry, include the time to ignition, t_{ign}; the heat release rate curve, and especially its peak value, the peak heat release rate, PHRR; the time to PHRR, t_{PHRR}; the mass loss rate, MLR; and the specific extinction area, SEA, a measure of the amount of smoke evolved. Generally, one expects a significantly reduced PHRR, typically on the order of 50% to 60% for montmorillonite-polystyrene nanocomposites, along with a reduced mass loss rate and a reduced time to ignition. The results for PS magadiite nanocomposites are shown in *Table 4*; the time to ignition is reduced, but there is essentially no change in any of the other parameters. The lack of a change in the PHRR is particularly surprising, since intercalated and exfoliated montmorillonite nanocomposites always show large changes in PHRR.

Based on this data, one can assert that there is a large difference between montmorillonite and magadiite polystyrene-clay nanocomposites. For montmorillonite,

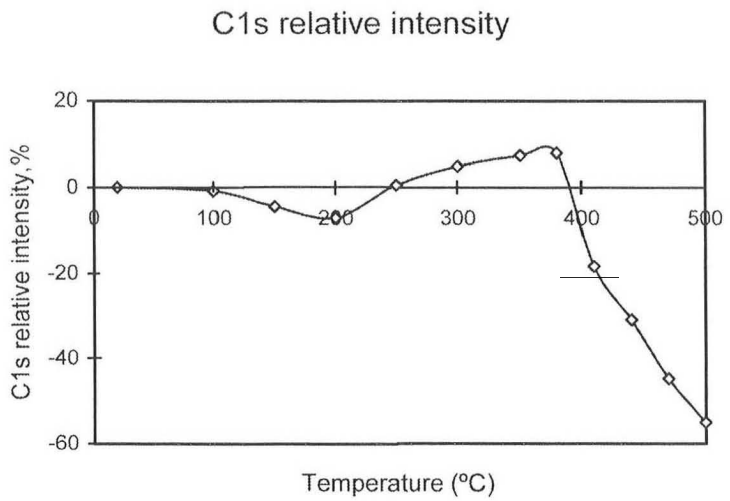

Fig. 10. Relative intensity in C1s spectra vs. temperature.

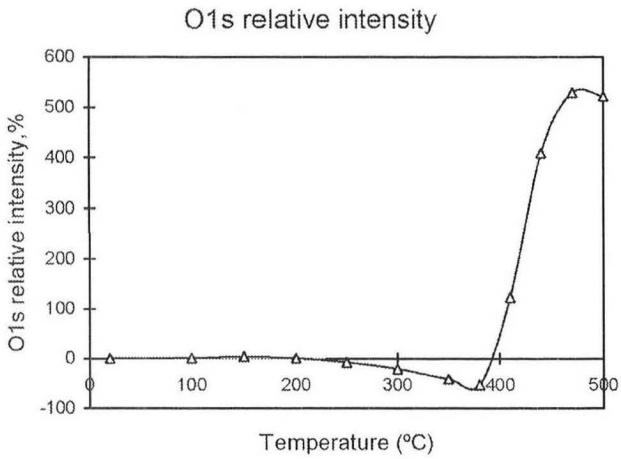

Fig. 11. Relative intensity in O1s spectra vs. temperature.

the onset temperature of the degradation is significantly enhanced and the PHRR is significantly reduced. On the other hand, for magadiite, neither of these changes occurs. Two other silicate-only clays, fluorohectorite (32) and hectorite (33), have been examined; for fluorohectorite there is no change in the PHRR, while with hectorite there is a change, but this is evident only at 5% clay, rather than 3% as in montmorillonite. Thus there are four systems to consider, montmorillonite in which a 50%–60% reduction in PHRR is observed at 3% clay; hectorite, in which the same reduction is observed but 5% clay is required; and fluorohectorite and magadiite, where there is no reduction in PHRR. For the first three clays there is no question that good nano-dispersion is obtained, while for magadiite, there is some question. The TEM images presented herein do not support excellent nano-dispersion but the enhanced mechanical properties do. In the discussion that follows, it is assumed that the nano-dispersion is good and possibilities are examined to explain the observations.

The differences between the various clays include: 1) dispersion, 2) composition, 3) location of charge in octahedral or tetrahedral layers, and 4) size of the individual clay platelets. As noted above, the assumption is made that all of the clays are well-dispersed in the polymer, so this cannot explain the effect that is observed, if the nano-dispersion of magadiite is not sufficient, this entire discussion should be discarded. There is a difference in composition, with one clay, montmorillonite, containing aluminum and the others having no aluminum. Since hectorite gives a reduction in PHRR and the other silicate only materials do not, composition cannot be the driving influence. It is possible that charge location is an important parameter, but this information is not accessible and thus this cannot be evaluated.

This leaves size as the important parameter to be considered. Hectorite is lathlike, while fluorohectorite is much more floppy and tends to fold onto itself to reduce the aspect ratio, and magadiite is very monolithic.

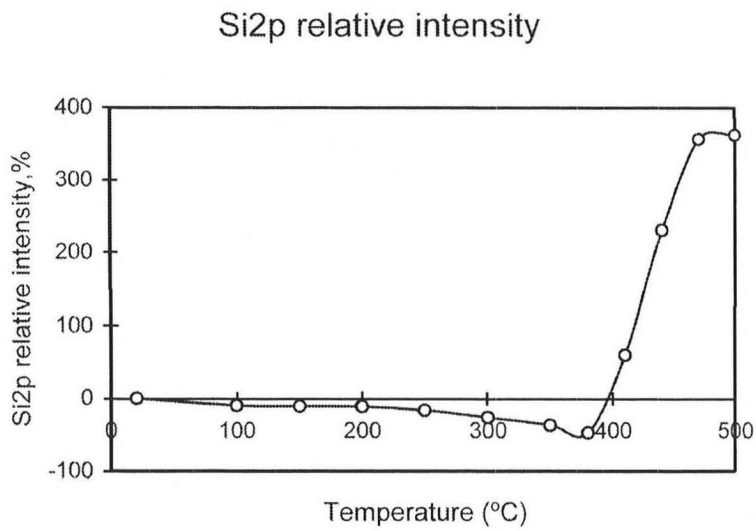

Fig. 12. Relative intensity in Si2p spectra vs. temperature.

Table 4. Cone Calorimetry Data for Magadiite PS (Nano)Composites.

Sample	t_{ign}, s	PHRR[a], kW/m²	t_{PHRR}, s	SEA[b], m²/kg	MLR[c], g/s.m²
PS	42	1021	91	1400	26
PS-Maga	23	1095	69	1391	26
PS-Mag-VB16, H_2O, 1×	27	897	70	1443	24
PS-Maga-VB16, THF, 1×	35	1094	81	1359	28

[a]PHRR: Peak Heat Release Rate.
[b]SEA: Specific Extinction Area, a measure of smoke.
[c]MLR: Mass Loss Rate.

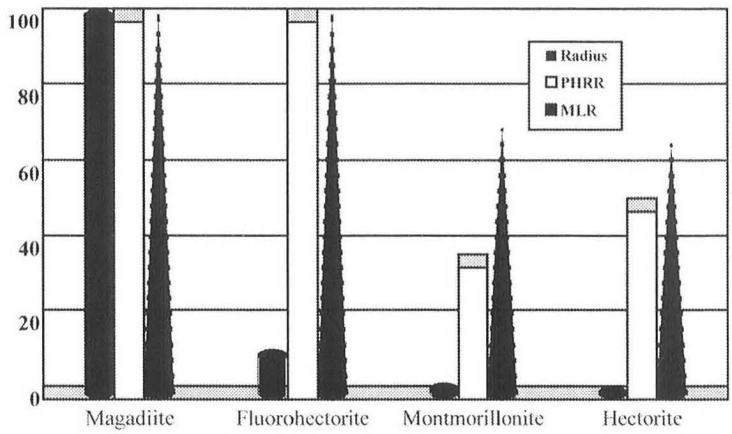

Fig. 13. Comparison, in order, of the radius of the individual clay platelet, the peak heat release rate (PHRR) and the mass loss rate (MLR) for four clays.

The plate diameter and aspect ratios of the clays under consideration are: Magadiite, plate diameter ~40 μm, (this is an average value that has been obtained from scanning electron microscopy that has been reported) (34); fluorohectorite, plate diameter, ~4–5 μm (32), 5 μm (35), aspect ratio, 500:1 to 4000:1 (32); montmorillonite, plate diameter, ~0.1–1 μm (32) 0.3–0.6 μm (35), 0.25 μm (36), aspect ratio, 100:1 to 1000:1 (32); hectorite, 0.05 μm (36), ~0.02–0.03 μm (37). There is a great variation in the sizes of the various clay particles and this size is plotted in *Fig. 13* against the reductions in PHRR and mass loss rate. It can be seen that there is a correlation.

The accepted process for reduction in PHRR is the formation of an impermanent barrier that prevents mass transfer and insulates the bulk polymer for some time (32). It is envisioned that the clay platelets fall and come into contact with each other, forming the barrier. Since they are only in contact, and not attached, the barrier is impermanent. The type of contact will be dependent upon the dimension of the clay platelets; if they are too small, it will take more to provide the necessary coverage, while if they are too large, they may not fall into a flat orientation, leaving a gap, that will permit the escape of volatiles and also the ingress of thermal energy.

CONCLUSIONS

Cation exchange is more difficult for magadiite than for clays with a lower cation exchange capacity and there is some solvent dependence on the exchange. The same organic-modification that was used in this study had been used previously with montmorillonite and this gave excellent nano-dispersion of the clay throughout the polymer. With magadiite, the dispersion is not as good, but it is apparent that there is at least partial nano-dispersion of the magadiite throughout the polystyrene. There is a better improvement in mechanical properties for this silicate clay than for the aluminosilicate systems. The improvement in mechanical properties suggests nano-dispersion. From XPS measurements, it is determined that the silicate does form a surface layer, just as seen with aluminosilicate clays, but this surface layer does not provide the barrier to prevent thermal degradation that is achieved with the aluminosilicates. TGA/FTIR shows that the presence of the clay does not change the degradation pathway in the same way that the aluminosilicate clays do. From cone calorimetry, there is no change in the peak heat release rate, indicating that the fire retardancy effects that have been attributable to nanocomposite formation are not present for this clay.

One may attribute the lack of a change in TGA and cone calorimetry to either the lack of nano-dispersion or to the difference among the clays, and the difference that has been particularly highlighted in this study is the variation in the dimensions of the individual clay platelets. Magadiite, and other clays that have a different dimension than does montmorillonite, may still have a role to play in fire retardancy, as one component of a multicomponent system. It is most likely that the clay alone will not provide the level of fire retardancy that is required but that the clay may serve to improve the mechanical properties such that the other components of the fire-retardant system can cause some deterioration in mechanical properties but the balance between all of the additives will lead to superior fire performance and useful mechanical properties.

ACKNOWLEDGMENT

Partial financial support from the U.S. Department of Commerce, National Institute of Standards and Technology, Grant Number 70NANB6D0119 is acknowledged. The authors are grateful to Prof. Barbara Silver-Thorn in College of Engineering, Marquette University, for the use of MTS machine.

REFERENCES

1. M. Alexandre and P. Dubois, *Mater. Sci. Eng.*, **R28**, 1 (2000).
2. E. P. Giannelis, R. Krishnamoorti, and E. Manias, *Adv. Polym. Sci.*, **138**, 107 (1999).
3. E. P. Giannelis, *Adv. Mater.*, **8**, 29 (1996).
4. R. A. Vaia, K. D. Jandt, E. J. Kramer, and E. P. Giannelis, *Chem. Mater.*, **8**, 2628 (1996).
5. D. A. Brune and J. Bicerano, *Polymer*, **42**, 369 (2002).
6. R. K. Bharadwaj, *Macromolecules.*, **34**, 9189 (2001).
7. G. Lagaly, K. Beneke, and A. Weiss, *Am. Mineral.*, **60**, 642 (1975).
8. K. Beneke and G. Lagaly, *Am. Mineral.*, **62**, 763 (1977).
9. K. Beneke and G. Lagaly, *Am. Mineral.*, **68**, 818 (1983).
10. Y. Sugahara, K. Sugimoto, T. Yanagisawa, Y. Nomizu, K. Kuroda, and D. Kato, *Yogyo Kyokai Shi*, **95**, 117 (1987).
11. Z. Wang, T. Lan, and T. J. Pinnavaia, *Chem. Mater.*, **8**, 2200 (1996).
12. T. J. Pinnavaia, I. D. Johnson, and M. J. Lipsicas, *Solid State Chem.*, **63**, 118 (1986).
13. J. M. Garces, S. C. Rocke, C. E. Crowder, and D. L. Hasha, *Clays Clay Miner.*, **36**, 409 (1988).
14. Y. Huang, Z. Jiang, and W. Schwieger, *Chem. Mater.*, **11**, 1210 (1999).
15. M.-J. Binette and C. Detellier, *Can. J. Chem.*, **80**, 1708 (2002).
16. K. Isoda, K. Kuroda, and M. Ogawa, *Chem. Mater.*, **12**, 1702 (2000).
17. Z. Wang and T. J. Pinnavaia, *Chem. Mater.*, **10**, 1820 (1998).
18. Z. Wang, T. Lau, and T. J. Pinnavaia, *Chem. Mater.*, **8**, 2200 (1996).
19. Y. Sugahara, K. Sugimoto, T. Yanagisawa, Y. Nomizu, and K. Kuroda, *Kato, Chuzo.*, **95**, 117 (1987).
20. M. Ogawa, T. Ishii, N. Miyamoto, and K. Kuroda, *Adv. Mater.*, **13**, 1107 (2001).
21. J. Zhu, A. B. Morgan, F. J. Lamelas, and C. A. Wilkie, *Chem. Mater.*, **13**, 3774 (2001).
22. D. Wang, J. Zhu, Q. Yao, and C. A. Wilkie, *Chem. Mater.*, **14**, 3837 (2002).
23. J. W. Gilman, T. Kashiwagi, M. Nyden, J. E. T. Brown, C. L. Jackson, and S. Lomakin, in *Chemistry and Technology of Polymer Additives*, pp. 249–65, S. Al-Malaika, A. Golovoy, and C. A. Wilkie, eds., Blackwell Scientific, London (1998).
24. J. Wang, J. Du, J. Zhu, and C. A. Wilkie, *Polym. Degrad. Stab.*, **77**, 249 (2002).
25. J. Du, J. Zhu, C. A. Wilkie, and J. Wang, *Polym. Degrad. Stab.*, **77**, 377 (2002).
26. J. Hao, S. Wu, C. A. Wilkie, and J. Wang, *Polym. Degrad. Stab.*, **66**, 81 (1999).
27. J. Hao, C. A. Wilkie, and J. Wang, *Polym. Degrad. Stab.*, **71**, 305 (2001).
28. S. Su and C. A. Wilkie, *Polym. Degrad. Stab.*, **83**, 347 (2004).
29. J. Wang, J. Du, J. Zhu, and C. A. Wilkie, *Polym. Degrad. Stab.*, **77**, 249 (2002).
30. J. Du, J. Zhu, C. A. Wilkie, and J. Wang, *Polym. Degrad. Stab.*, **77**, 377 (2002).
31. J. W. Gilman, *Appl. Clay Sci.*, **15**, 31 (1999).
32. J. W. Gilman, C. L. Jackson, A. B. Morgan, R. Harris Jr., E. Manias, E. P. Giannelis, M. Wuthenow, D. Hilton, and S. H. Phillips, *Chem. Mater.*, **12**, 1866 (2000).
33. D. Wang, B. N. Jang, S. Su, J. Zhang, X. Zheng, G. Chigwada, D. D. Jiang, and C. A. Wilkie, in *Fire Retardancy of Polymers: The use of mineral fillers in micro- and nano-composites*, M. Le Bras, S. Bourbigot, S. Duquesne, C. Jama, and C. Wilkie, eds., Royal Society of Chemistry, Cambridge, in press.
34. J. S. Dailey and T. J. Pinnavaia, *Chem. Mater.*, **4**, 855 (1992). H. O. Pastore, M. Munsignatti, and A. J. S. Mascarenhas, *Clay and Clay Minerals*, **48**, 224 (2000). K. Isoda, K. Kuroda, and M. Ogawa, *Chem. Mater.*, **12**, 1702 (2000). K. Kikuta, K. Ohta, and K. Takagi, *Chem. Mater.*, **14**, 3123 (2002).
35. J. Ren, B. F. Casanueva, C. A. Mitchell, and R. Krishnamoorti, *Macromolecules*, **36**, 4188 (2003).
36. S.-S. Hou and K. Schmidt-Rohr, *Chem. Mater.*, **15**, 1938 (2003).
37. T. Kasawa, T. Murakami, N. Kohyama, and T. Watanabe, *Am. Mineralogist*, **86**, 105 (2001).